

## Luminescent CdSe/CdS Core/Shell Nanocrystals in Dendron Boxes: Superior Chemical, Photochemical and Thermal Stability

Wenzhuo Guo, J. Jack Li, Y. Andrew Wang, and Xiaogang Peng\*

Contribution from the Department of Chemistry and Biochemistry, University of Arkansas, Fayetteville, Arkansas 72701

Received September 9, 2002; E-mail: xpeng@comp.uark.edu

**Abstract:** The surface ligands, generation-3 (G3) dendrons, on each semiconductor nanocrystal were globally cross-linked through ring-closing metathesis (RCM). The global cross-linking of the dendron ligands sealed each nanocrystal in a dendron box, which yielded box-nanocrystals. Although the dendron ligands coated CdSe nanocrystals (CdSe dendron-nanocrystals) were already quite stable, the stability of CdSe box-nanocrystals against chemical, photochemical, and thermal treatments were dramatically improved in comparison to that of the original dendron-nanocrystals. Furthermore, the box structure of the ligands monolayer coupled with the stable inorganic CdSe/CdS core/shell nanocrystals resulted in a class of extremely stable nanocrystal/ligands complexes. The band edge photoluminescence of the core/shell dendron-nanocrystals and box-nanocrystals were partially remained, and could be further brightened through controlled chemical oxidation or photooxidation. Practically, the stability of the box-nanocrystals is sufficient for most fundamental studies and technical applications. The box-nanocrystals may represent a general solution for the commonly encountered instability for many types of colloidal nanocrystals. The size distribution of the empty dendron boxes formed by the dissolution of the inorganic nanocrystals in concentrated HCl was very narrow. The empty boxes as new types of polymer capsules are soluble in solution, mesoporous, and with a very thin but stable peripheral. Those nanometer-sized cavities should be of interest for many purposes in the field of solution host-guest chemistry.

### Introduction

Colloidal nanocrystals are of great interest for both fundamental studies<sup>1–4</sup> and technical applications<sup>5–11</sup> due to their interesting size dependent properties.<sup>1,2</sup> Many current research activities in the field of colloidal nanocrystals are strongly hindered by the availability of desired quality nanocrystals<sup>12,13</sup> and reliable processing chemistry,<sup>14,15</sup> especially the latter. The recent rapid progress on synthesis of high quality nanocrystals,

including semiconductor,<sup>16–23</sup> metal,<sup>24–26</sup> and oxide<sup>27–31</sup> systems, has put the processing chemistry on an even more urgent position. As pointed out previously,<sup>14,15</sup> the processing chemistry of colloidal nanocrystals is mostly related to the nature and structure of the surface ligands monolayer, the interface between the inorganic core and the organic ligands monolayer, and the structure of the surface of the inorganic nanocrystals. Unfortunately, knowledge on those issues is limited at present.<sup>14,15</sup>

- (1) Brus, L. J. *J. Phys. Chem.* **1986**, *90*, 2555–60.
- (2) Alivisatos, A. P. *Science* **1996**, *271*, 933–937.
- (3) Heath, J. R., Ed. *Acc. Chem. Res.* **1999**, *Special Issue for Nanostructures*, review articles relevant to colloidal nanocrystals.
- (4) Empedocles, S. A.; Neuhäuser, R.; Shimizu, K.; Bawendi, M. G. *Adv. Mater.* **1999**, *11*, 1243–1256.
- (5) Schlamp, M. C.; Peng, X. G.; Alivisatos, A. P. *J. Appl. Phys.* **1997**, *82*, 5837–5842.
- (6) Mattoussi, H.; Radzilowski, L. H.; Dabbousi, B. O.; Thomas, E. L.; Bawendi, M. G.; Rubner, M. F. *J. Appl. Phys.* **1998**, *83*, 7965–7974.
- (7) Greenham, N. C.; Peng, X. G.; Alivisatos, A. P. *Phys. Rev. B* **1996**, *54*, 17 628–17 637.
- (8) Bruchez, M.; Moronne, M.; Gin, P.; Weiss, S.; Alivisatos, A. P. *Science* **1998**, *281*, 2013–2016.
- (9) Taton, T. A.; Mirkin, C. A.; Lesinger, R. L. *Science* **2000**, *289*, 1757.
- (10) Chan, W. C. W.; Nie, S. M. *Science* **1998**, *281*, 2016–2018.
- (11) Klimov, V. I.; Mikhailovsky, A. A.; Xu, S.; Malko, A.; Hollingsworth, J. A.; Leatherdale, C. A.; Eisler, H. J.; Bawendi, M. G. *Science* **2000**, *290*, 314–317.
- (12) Murray, C. B.; Kagan, C. R.; Bawendi, M. G. *Annu. Rev. Mater. Sci.* **2000**, *545*.
- (13) Peng, X. *Chem. Eu. J.* **2002**, *8*, 334–339.
- (14) Wang, Y. A.; Li, J. J.; Chen, H.; Peng, X. *J. Am. Chem. Soc.* **2002**, *124*, 2293–2298.
- (15) Aldana, J.; Wang, Y.; Peng, X. *J. Am. Chem. Soc.* **2001**, *123*, 8844.

- (16) Murray, C. B.; Norris, D. J.; Bawendi, M. G. *J. Am. Chem. Soc.* **1993**, *115*, 8706–8715.
- (17) Peng, X.; Wickham, J.; Alivisatos, A. P. *J. Am. Chem. Soc.* **1998**, *120*, 5343–5344.
- (18) Peng, X.; Manna, L.; Yang, W. D.; Wickham, J.; Scher, E.; Kadavanich, A.; Alivisatos, A. P. *Nature* **2000**, *404*, 59–61.
- (19) Peng, Z. A.; Peng, X. *J. Am. Chem. Soc.* **2001**, *123*, 183–184.
- (20) Peng, Z. A.; Peng, X. *J. Am. Chem. Soc.* **2002**, *124*, 3343–3353.
- (21) Qu, L.; Peng, Z. A.; Peng, X. *Nano Lett.* **2001**, *1*, 333.
- (22) Qu, L.; Peng, X. *J. Am. Chem. Soc.* **2002**, *124*, 2049–2055.
- (23) Yu, W. W.; Peng, X. *Angew. Chem., Inter. Ed.* **2002**, *41*, 2368–2371.
- (24) Brust, M.; Walker, M.; Bethell, D.; Schiffrin, D. J.; Whyman, R. *Chem. Commun.* **1994**, 801–802.
- (25) Lin, X. M.; Sorensen, C. M.; Klabunde, K. J. *J. Nanopart. Res.* **2000**, *2*, 157–164.
- (26) Whetten, R. L.; Shafiqullin, M. N.; Khoury, J. T.; Schaaff, T. G.; Vezmar, I.; Alvarez, M. M.; Wilkinson, A. *Acc. Chem. Res.* **1999**, *32*, 397.
- (27) Trentler, T. J.; Denler, T. E.; Bertone, J. F.; Agrawal, A.; Colvin, V. L. *J. Am. Chem. Soc.* **1999**, *121*, 1613–1614.
- (28) Rockenberger, J.; Scher, E. C.; Alivisatos, A. P. *J. Am. Chem. Soc.* **1999**, *121*, 11 595–11 596.
- (29) O'Brien, S.; Brus, L.; Murray, C. B. *J. Am. Chem. Soc.* **2001**, *123*, 12 085–12 086.
- (30) Sun, S.; Zeng, H. *J. Am. Chem. Soc.* **2002**, *124*, 8204–8205.
- (31) Pacholski, C.; Kornowski, A.; Weller, H. *Angew. Chem., Int. Ed. Engl.* **2002**, *41*, 1188–1191.

However, it is evidenced that the technical key challenge of the processing chemistry of colloidal nanocrystals is to obtain stable nanocrystal/ligands complexes. It is not difficult to find evidences in the literature which support this statement. The lifetime of the light emitting diodes (LEDs) based on semiconductor nanocrystals was short,<sup>5</sup> which is likely a result of the dissociation of the organic ligands from the nanocrystals due to the thermal effects of the devices in operation. The troublesome conjugation chemistry related to the promising biological labeling using semiconductor nanocrystals has been also found to be associated with the detachment of the organic ligands from the nanocrystals.<sup>14,15</sup> The long-pursued enhancement effect of magnetic nanocrystals for magnetic resonance imaging is still in its infancy because of the instability of the ligands on the surface of the nanocrystals.<sup>32,33</sup> It would be very interesting to study the chemical reactivity of colloidal nanocrystals in solution if the ligands can stabilize the initial nanocrystals, the intermediates and the resulting nanocrystals.

Two types of stability issues related to nanocrystal/ligands complexes have been identified. Type I, the organic ligands dissociate from the inorganic core. In solution, this results in uncontrollable chemical properties of the outer surface of the ligands monolayer and the detachment of the desired chemical/biochemical functions from the inorganic core.<sup>15</sup> In many cases, this also causes the precipitation of the nanocrystals. In both solid state and solution phase, the dissociation of the organic ligands and the inorganic core often causes undesired variations of the properties of nanocrystals, such as decrease of either photoluminescence<sup>22</sup> or electroluminescence<sup>5</sup> brightness. Type II, the inorganic core can be oxidized, etched, and even completely dissolved, which normally defeats the function of the original nanocrystal/ligands complexes.

This work intended to stabilize nanocrystal/ligands complexes by improving the stability of both inorganic core and the organic ligands monolayer, with an emphasis on the latter. Semiconductor nanocrystals were chosen because of their general interest, easy detection and relatively better established synthetic and ligands chemistry. The stability of CdSe nanocrystal cores was enhanced by the epitaxial growth of a thin layer of CdS on their surface.<sup>34,35</sup> It was confirmed that such core/shell structures can improve the photochemical stability of CdSe nanocrystals by the confinement of the photogenerated charges inside the core material.<sup>34,35</sup> The stability enhancement of the ligands monolayer was achieved by the cross-linking of all surface ligands of each nanocrystal through the standard ring-closing metathesis (RCM). To reach the desired global cross-linking, a generation 3 (G3) dendron with thiol as the anchoring group and eight carbon-carbon double bond as the terminal groups was employed as the surface ligands. The relatively good chemical stability of the dendron ligands coated nanocrystals (dendron-nanocrystals)<sup>14</sup> enabled the nanocrystal/ligands complexes to readily survive the cross-linking reaction and related purification procedures. The multiple double bonds of each dendron ligand made it possible to obtain global cross-linking of all the dendron ligands

on the surface of each nanocrystal through RCM<sup>36-38</sup> to form a dendron box around each nanocrystal (box-nanocrystal). The formation of the dendron boxes was confirmed by NMR and MS. The chemical, photochemical and thermal stability of the resulting box-nanocrystals were quantitatively or semiquantitatively examined. High quality CdSe/CdS core/shell box-nanocrystals demonstrated superior stability against HCl etching, chemical oxidation with H<sub>2</sub>O<sub>2</sub>, photochemical oxidation, and thermal sintering. The resulting stable semiconductor nanocrystals should be of great interest for many fundamental studies, such as measurement of the sized dependent melting point of nanocrystals and studies on the size-specified reactivity of nanocrystals. Furthermore, those luminescent and stable core/shell nanocrystals should greatly benefit several types of technical applications, such as light emitting diodes (LEDs),<sup>5,6</sup> solid-state lasers,<sup>11</sup> and biological labeling,<sup>8,10,11</sup> and so forth. The empty dendron boxes formed by the dissolution of the inorganic nanocrystals in concentrated HCl represent a new class of nanometer sized polymer capsules, which are nearly monodisperse, soluble, stable, and with a very thin peripheral.

## Experimental Section

**Chemicals.** Triphenylmethanol, 2-aminoethanethiol hydrochloride, bromoacetyl bromide, diallyl amine, triethylsilane, trifluoroacetic acid (TFA), tetramethylammonium hydroxide, trioctylphosphine oxide (TOPO, technical grade, 90%), trioctylphosphine (TOP, technical grade, 90%) cadmium acetate hydrate (99.99+%), selenium powder (100 mesh, 95%), anhydrous toluene (99.8%), diatomaceous earth, Grubbs' catalyst (second generation) were purchased from Aldrich. Anhydrous ethyl ether, benzene, chloroform, *N,N*-dimethylformamide (DMF), acetone, ethyl acetate, methanol, triethylamine, and K<sub>2</sub>CO<sub>3</sub>, were purchased from EM science. All chemicals were used directly without further purification.

**Synthesis of Dendron Ligands.** G3 dendron ligand **6** was synthesized as shown in Scheme 1. The focal point of the dendron ligands, a thiol group, was the binding site to surface cadmium atoms of the nanocrystals. In the synthesis, triphenylmethyl group was applied to protect thiol group. With this protection, dendron precursors were stable under both acidic and basic conditions. Generally, compound **2**, 2-tritylsulfanyl-ethylamine was obtained upon the treatment of triphenylmethanol with 2-aminoethanethiol hydrochloride in TFA, followed by neutralization with aqueous NaOH. The acetonitrile solution of **2** was refluxed with *N*-(*tert*-Butoxycarbonyl)aziridine to give *tert*-butoxycarbonyl (BOC) protected first generation of dendron. Compound **3** was obtained as yellow oil after the deprotection of BOC groups with TFA. Reaction of bromoacetyl bromide with diallyl amine at 0 °C afforded compound **4**, *N,N*-diallyl-2-bromo-acetamide. The triphenylmethyl protected G3 dendron ligand was readily prepared by *N*-alkylation of compound **3** with active  $\alpha$ -bromide **4** in the presence of aqueous K<sub>2</sub>CO<sub>3</sub>. Dendron ligand **6** was finally obtained by treatment **5** with TFA and triethylsilane.

**2-Tritylsulfanyl-ethylamine (2).** Triphenylmethanol (22.9 g, 88 mmol) was added to a solution of 2-aminoethanethiol hydrochloride (10 g, 88 mmol) in trifluoroacetic acid (TFA, 40 mL). The result solution was stirred at room temperature for about 40 min. TFA was removed under reduced pressure. The residue was triturated with ethyl ether. The white precipitate formed was filtered, partitioned with aqueous NaOH (40 mL, 1 N) and extracted with ethyl acetate (3 × 50 mL). The combined organic layers were dried over Na<sub>2</sub>SO<sub>4</sub>. The product

(32) Wunderbaldinger, P.; Bogdanov, A., Jr.; Weissleder, R. *Eu. J. Radiology* **2000**, *34*, 156.

(33) Weissleder, R. *Radiology* **1999**, *212*, 609-614.

(34) Peng, X.; Schlamp, M. C.; Kadavanich, A. V.; Alivisatos, A. P. *J. Am. Chem. Soc.* **1997**, *119*, 7019-7029.

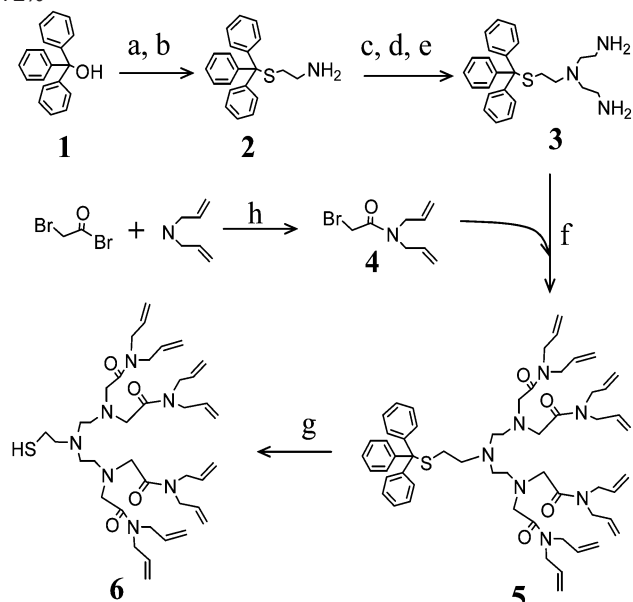
(35) Li, J.; Wang, Y. A.; Peng, X.; Guo, W.; Mishima, T.; Johnson, M., submitted.

(36) Wendland, M. S.; Zimmerman, S. C. *J. Am. Chem. Soc.* **1999**, *121*, 1389-1390.

(37) Hecht, S.; Frechet, M. J. *Angew. Chem. Int. Ed.* **2001**, *40*, 74.

(38) Zimmerman, S. C.; Wendland, M. S.; Rakow, N. A.; Zharov, I.; Suslick, K. S. *Nature* **2002**, *418*, 399-403.

**Scheme 1.** Synthesis of Dendron Ligand. Reagent and Condition: A, 2-aminoethanethiol Hydrochloride, TFA, 25 °C, 30 min, 85%; B, 1 M NaOH, 96%; C, *N*-(*tert*-Butoxycarbonyl)aziridine, CH<sub>3</sub>CN, Reflux 3 days, 67%; D, TFA, 30 Mins, 92%; E, 1 M NaOH, 98%; F, THF, K<sub>2</sub>CO<sub>3</sub>, Reflux, 12 Hours, 62%; G, TFA, Triethylsilane, 95%; H, Ethyl Acetate, 72%



was obtained as white solid after solvent evaporation (23.8 g, yield: 85%). ESI-MS ( $m/z$ ): 320 ( $M + H^+$ ). <sup>1</sup>H NMR  $\delta_D$  (CDCl<sub>3</sub>): 7.21~7.43 (m, 15H, pheny), 2.58 (t, 2H, SCH<sub>2</sub>), 2.32 (t, 2H, CH<sub>2</sub>N). <sup>13</sup>C NMR  $\delta$ : 144.98, 129.68, 127.94, 126.73, 66.63, 41.15, 36.38. Anal. Calcd for C<sub>21</sub>H<sub>21</sub>NS: C, 78.95; H, 6.63; N, 4.38. Found: C, 77.90; H, 6.57; N, 4.35.

**Bis-(2-amino-ethyl)-(2-tritylsulfanyl)-amine (3).** The CH<sub>3</sub>CN (135 mL) solution of compound 2 (9.3 g, 29 mmol) and *N*-(*tert*-butoxycarbonyl)aziridine (12.3 g, 87 mmol) was refluxed for 3 day. The solvent was removed under reduced pressure. The residue oil was purified by silica gel column chromatography with CHCl<sub>3</sub> as eluent to obtain 12.3 g of BOC protected G1 dendron as light yellow solid which was treated with TFA, dried under reduced pressure, partitioned with aqueous NaOH to give compound 3 as yellow oil (7.9 g, yield: 68%). ESI-MS ( $m/z$ ): 406 ( $M + H^+$ ). <sup>1</sup>H NMR  $\delta_D$  (CDCl<sub>3</sub>): 7.23~7.44 (m, 15H, phenyl), 2.78 (t, 2H, SCH<sub>2</sub>), 2.60~2.70 (m, 4H, CH<sub>2</sub>NH<sub>2</sub>), 2.27~2.35 (m, 6H, CH<sub>2</sub>N). <sup>13</sup>C NMR  $\delta$ : 145.00, 129.68, 127.92, 126.67, 66.80, 56.61, 53.32, 39.62, 30.23. Anal. Calcd for C<sub>25</sub>H<sub>31</sub>N<sub>3</sub>S: C, 74.03; H, 7.70; N, 10.36. Found: C, 73.56; H, 7.32; N, 9.78.

***N,N*-Diallyl-2-bromoacetamide (4).** Bromoacetyl bromide (45 g, 0.22 mol) in ethyl acetate (25 mL) was added dropwise to a solution of diallyl amine (9.6 g, 0.1 mol), Et<sub>3</sub>N (15 mL), in ethyl acetate (50 mL) at 0 °C. The reaction was then warmed to ambient temperature, and the stirring was continued for 3 h. The resulting mixture was washed with saturated NaHCO<sub>3</sub> solution (3 × 100 mL), dried over Na<sub>2</sub>SO<sub>4</sub>. The evaporation of the solvent give 16.2 g product as light yellow oil (yield: 75%). ESI-MS ( $m/z$ ): 218 ( $M + H^+$ ). <sup>1</sup>H NMR  $\delta_D$  (CDCl<sub>3</sub>): 5.75 (m, 2H, CH), 5.19 (m, 4H, CH<sub>2</sub>), 3.95 (d, 4H, NCH<sub>2</sub>), 3.81 (2, 2H, BrCH<sub>2</sub>). <sup>13</sup>C NMR  $\delta$ : 166.89, 132.64, 132.21, 117.66, 117.21, 50.10, 48.23, 26.24. Anal. Calcd for C<sub>8</sub>H<sub>12</sub>BrNO: C, 44.06; H, 5.55; N, 6.42. Found: C, 43.33; H, 5.65; N, 6.26.

***N,N*-Diallyl-2-({2-[[2-bis-diallylcarbamoymethyl-amino)-ethyl]-2-tritylsulfanyl-ethyl-amino)-ethyl}-daillylcarbamoymethyl-amino)-acetamide (5).** compound 4 (0.9 g, 4.1 mmol) was added to a solution of 3 (0.4 g, 1 mmol), K<sub>2</sub>CO<sub>3</sub> (0.84 g, 6 mmol, in 3 mL H<sub>2</sub>O) in THF (15 mL). The reaction mixture was heated at 65 °C overnight. The solvent was removed under reduced pressure. The residue was purified by silica gel column chromatography eluted with CHCl<sub>3</sub>/MeOH

(85/15) to obtain light yellow product (0.7 g, yield: 73%). ESI-MS ( $m/z$ ): 954 ( $M + H^+$ ). <sup>1</sup>H NMR  $\delta_D$  (CDCl<sub>3</sub>): 7.21~7.33 (m, 15H, phenyl), 5.68 (m, 8H, CH), 5.07 (m, 16H, CHCH<sub>2</sub>), 3.44~3.88 (m, 24H, COCH<sub>2</sub>, CH<sub>2</sub>CHCH<sub>2</sub>), 2.81 (m, 2H, SCH<sub>2</sub>), 2.31 (m, 10H, NCH<sub>2</sub>). <sup>13</sup>C NMR  $\delta$ : 170.02, 144.98, 133.21, 133.14, 129.67, 127.98, 126.63, 117.46, 116.57, 66.58, 55.31, 53.91, 48.70, 47.82, 30.24. Anal. Calcd for C<sub>57</sub>H<sub>75</sub>N<sub>7</sub>O<sub>4</sub>S: C, 71.74; H, 7.92; N, 10.27. Found: C, 70.96; H, 7.37; N, 10.41.

***N,N*-Diallyl-2-({2-[[2-bis-diallylcarbamoymethyl-amino)-ethyl]-2-mercapto-ethyl-amino)-ethyl}-diallylcarbamoymethyl-amino)-acetamide (6).** Triethylsilane (0.1 mL) was added to a solution of 5 (0.5 g, 0.5 mmol) in trifluoroacetic acid (10 mL). A white precipitate formed upon the addition was removed by filtration through diatomaceous earth. TFA was removed under reduced pressure to give product as light yellow oil (0.34 g, 95%). ESI-MS ( $m/z$ ): 712 ( $M + H^+$ ). <sup>1</sup>H NMR  $\delta_D$  (CDCl<sub>3</sub>): 5.68 (m, 8H, CH), 5.07 (m, 16H, CHCH<sub>2</sub>), 3.44~3.88 (m, 24H, COCH<sub>2</sub>, CH<sub>2</sub>CHCH<sub>2</sub>), 2.75 (m, 2H, SCH<sub>2</sub>), 2.31 (m, 10H, NCH<sub>2</sub>). <sup>13</sup>C NMR  $\delta$ : 170.21, 133.05, 132.90, 117.48, 116.57, 68.52, 58, 13, 55.47, 48.57, 47.92, 28.71. Anal. Calcd for C<sub>38</sub>H<sub>61</sub>N<sub>7</sub>O<sub>4</sub>S: C, 64.10; H, 8.64; N, 13.77. Found: C, 63.25; H, 8.49; N, 13.44.

**Synthesis of CdSe and CdSe/CdS Nanocrystals.** TOPO-capped or amine-capped CdSe nanocrystals were synthesized using the standard "greener" methods reported previously.<sup>15,21,22</sup> The typical size of the nanocrystals used in this work was about 3.3 nm with the first excitonic absorption peak at 550 nm. The CdSe/CdS core/shell nanocrystals were synthesized through the newly developed solution atomic layer epitaxy (SALE) method<sup>35</sup> which will be reported later. The core size of the core/shell nanocrystals was about 3.5 nm and the shell thickness was about 1.5 monolayers of CdS.

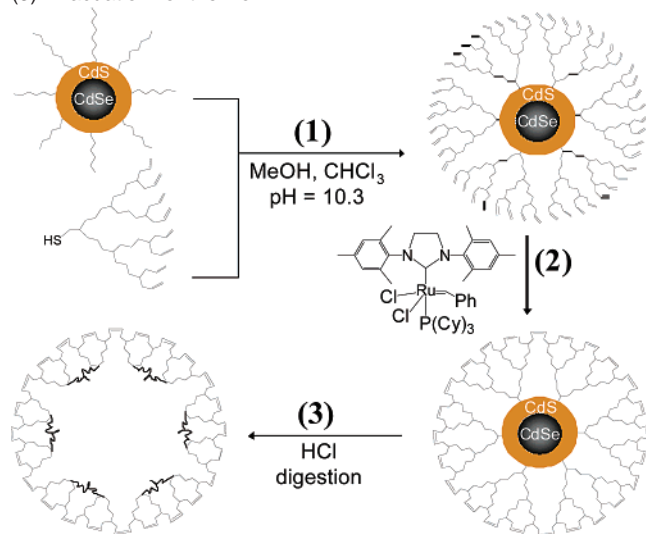
**Surface Modification of Nanocrystal with Dendron Ligands.** CdSe and CdSe/CdS core/shell nanocrystals were modified with dendron ligand 6 through a procedure modified from a previously reported one.<sup>14,15</sup> Typically, 20 mg of TOPO-capped CdSe nanocrystals in CHCl<sub>3</sub> was added to a solution of 150 mg ligand in 15 mL of 1:1 ratio MeOH/CHCl<sub>3</sub>, and the pH value of such solution was adjusted to 10.3 by the addition of tetramethylammonium hydroxide. The reaction was carried out under dark at room temperature or elevated temperatures overnight. In case of primary amine-coated CdSe/CdS core/shell nanocrystals, the basic solution of ligand and nanocrystals was first set to reflux under nitrogen for 4 h, and then the solution was cooled to room temperature and stirred for 12 h. The resulting dendron-nanocrystals were precipitated with minimum amount of ethyl ether, separated by centrifugation and decantation.

**Formation of Box-Nanocrystals.** The terminal allyl groups of the dendron-nanocrystals were cross-linked to form dendron-nanocrystals using Grubbs' ruthenium alkylidene catalyst (Scheme 2). Typically, the second generation of Grubbs' catalyst<sup>36,38</sup> (2 mol % per alkene group) was added to a 1:1 ratio CH<sub>2</sub>Cl<sub>2</sub>/benzene solution (10<sup>-5</sup> M, based on alkene group) of the dendron-nanocrystals. The amount of ligands on the surface of nanocrystals was estimated by assuming a close packing of ligands on the surface of nanocrystals. The reaction was carried out at room temperature for 48 h under dark. DMSO (20  $\mu$ l) and silica gel (0.5 g) were added to the reaction solution to remove the catalyst by a standard protocol. The box-nanocrystals were then precipitated out with minimum amount of ethyl ether, separated by centrifugation and decantation.

**Characterization of Box-Nanocrystals and Empty Dendron Boxes.** For the NMR studies, 20 mg of nanocrystals before and after cross-linking were dissolved /precipitated in the suitable solvents system, separated by centrifugation and decantation at least three times. After drying under high vacuum, the resulting samples were dissolved in DMSO (*d*<sub>6</sub>) and measured with a JEOL 270 MHz NMR spectrophotometer.

For the mass spectroscopy, the dendron-nanocrystals and the box-nanocrystals were digested by HCl. To do so, the nanocrystals were

**Scheme 2.** (1) Surface Ligands Exchange to Form Dendron-nanocrystals, (2) Formation of Box-nanocrystal, and (3) "Evacuation" of the Box



dissolved in DMF, then concentrated HCl was added. A colorless solution was obtained after 3 days. The clear solution was extracted with benzene, concentrated and detected with MALDI-TOF mass spectroscopy (Bruker Reflex III) using dihydrobenzoic acid as the matrix.

**Chemical, Thermal and Photochemical Stability of Box-Nanocrystals.** Two types of chemical stabilities of nanocrystals were investigated, i.e., HCl etching and  $\text{H}_2\text{O}_2$  oxidation. In a typical HCl etching experiment, HCl (0.4 mL, 0.2 M) was added to a cuvette containing 0.6 mL nanocrystals DMF solution (the initial optical density (OD) at the first absorption peak was adjusted to  $\sim 0.5$ ). The UV-vis spectra were recorded at a certain time interval until the solution became turbid. The  $\text{H}_2\text{O}_2$  oxidation experiments were carried out similarly to the HCl etching, but with  $\text{H}_2\text{O}_2$  (0.1 mL, 3 wt. % in water) as oxidant.

The thermal stability was examined by sintering the nanocrystals. The nanocrystal samples were dissolved and precipitated with suitable solvent system at least three times. The samples were then placed in a vacuum oven and dried for 2 h prior to heating. The oven temperature was raised to  $100\text{ }^\circ\text{C}$  and kept that temperature for about 60 min. After the oven was cooled to ambient temperature, the solubility of the resulting fine powder was tested, and the UV-vis absorption spectra of the solutions were recorded.

The photochemical stability of the nanocrystals was studied following the previously reported procedure.<sup>14,15</sup> The nanocrystals were dissolved in DMF, and the optical density (OD) was adjusted to  $\sim 0.3$  at the first absorbance peak. The small vials containing the samples were placed  $\sim 4$  cm under the ultraviolet lamp (UVP model UVGL-25 multiband). The lamp was set to 254 nm (short wavelength). The UV-vis absorption was monitored at certain time interval. The normalized OD at the original excitation absorption peak was used as the indicator of the photooxidation of the inorganic nanocrystals.<sup>14,15</sup>

## Results

The CdSe/CdS core/shell nanocrystals were synthesized through the newly developed solution atomic layer epitaxy (S-ALE) using cadmium oleate and elemental sulfur as the precursors.<sup>35</sup> The surface of the as-prepared core/shell nanocrystals was coated with primary amines. The CdSe core nanocrystals used in this study were synthesized using standard methods and coated with TOPO and/or primary amines as the surface ligands.<sup>15,21,22</sup>

The absorption spectra of both plain core and core/shell nanocrystals did not change upon the surface replacement of

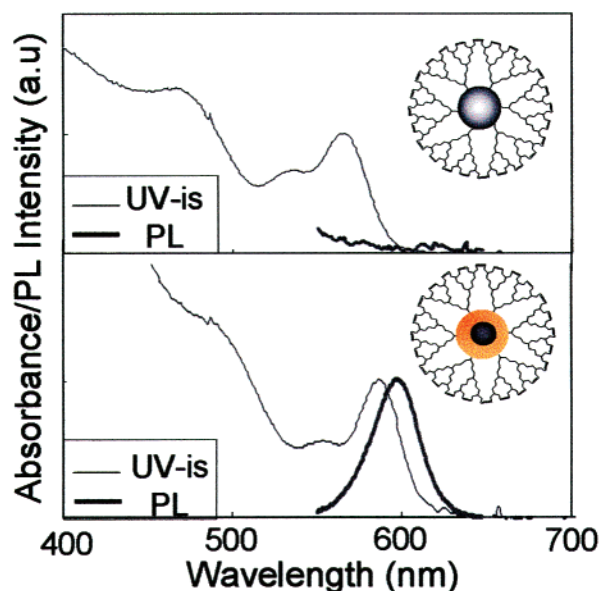


**Figure 1.** UV-vis and PL spectra of CdSe core and CdSe/CdSe core/shell box-nanocrystals.

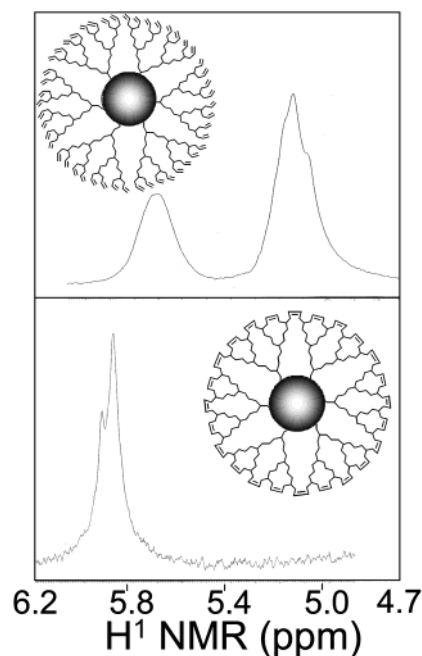


**Figure 2.** NMR spectra before and after the cross-linking reaction.

the original ligands by the thiol-based dendron ligands. The photoluminescence (PL) of the core nanocrystals was completely quenched.<sup>15</sup> On the contrast, the PL of the core/shell nanocrystals was partially remained as observed previously.<sup>8</sup> The optical spectra of the nanocrystals after the surface replacement were the same as the ones shown in Figure 1, which are the ones for the corresponding box-nanocrystals.  $^1\text{H}$ NMR results revealed the complete replacement of the original ligands by the thiol dendrons.

**Formation of a Dendron Box around each Nanocrystal: Box-Nanocrystals.** The typical RCM worked well for the cross-linking of the double bonds at the outer surface of the dendron ligands monolayer.<sup>1</sup>  $^1\text{H}$  NMR spectra (Figure 2) revealed that the original double bonds of the dendron ligands were out of the detection limit and the formation of the new double bonds through the cross-linking was readily observed.

The cross-linking process did not affect either PL or absorption properties of both types of nanocrystals (Figure 1). However, the solubility of the nanocrystals after the cross-linking varied significantly from that of the original dendron-nanocrystals. The original dendron-nanocrystals were soluble in typical nonpolar organic solvents, but the cross-linked nanocrystals were only soluble in aromatic solvents or polar organic solvents, such as benzene, DMSO, and DMF. The solubility of the box-nanocrystals was considered to be consistent with the resulting structures of the cross-ring metathesis.

Because each G3 dendron ligand has eight double bonds as its terminal groups (Schemes 1 and 2), it was expected that the complete cross-linking proven by the NMR measurements should form a “global” network of all ligands on the surface of each nanocrystal. In fact, typical dendrimer boxes reported in the literature were generally based on G3 dendrimers.<sup>36,38,39</sup> To prove this hypothesis, the nanocrystals after the cross-linking reaction were digested by concentrated HCl solution, which completely dissolved the CdSe nanocrystals. The clear and colorless solution was examined with  $^1\text{H}$ NMR and only broad peaks similar to the ones shown in Figure 2 (bottom) were detected. This result indicates that the ligands shell was still remain as large species in the solution after the removal of the center inorganic core.

The strong evidence of the expected “global” cross-linking of all dendron ligands of a given nanocrystal was given by the Mass spectroscopy measurements with the clear solution obtained by the HCl digestion. As shown in Figure 3. Before the cross-linking, only the dendron ligands in the digestion solution were detected by Mass spectroscope. However, after the cross-linking, a distinguishable peak with a very high molecular mass dominated the spectrum. Typically, the related mass of the peak observed after the cross-linking corresponded to about 15 to 50 dendron units with a full width at half-maximum as 2 to 5 dendron units. This number was compared to the values measured by the gravimetric method before digestion (see next paragraph) and a good agreement between these two methods was obtained.

The average number of the dendron units on the surface of each box-nanocrystal before digestion were obtained as follows. Nanocrystals after the cross-linking were carefully purified and the purity was examined by  $^1\text{H}$  NMR. Typically, if any free small molecules existed in the solution, very sharp and intense NMR signals would be detected. Certain amount of the purified nanocrystals in the form of fine powder was weighed to determine the total mass of the nanocrystal/ligands complexes, and then, those nanocrystals were dispersed in a known-volume solvent. The total number of inorganic nanocrystals in the solution was determined by the absorbance of the solution and the absorption extinction coefficient of the nanocrystals using Beer's Law,<sup>40</sup> and the size of the CdSe nanocrystal core was determined by the first peak of the absorption spectrum. With the above information, the average number of the dendron units per nanocrystal could be easily calculated.

The agreement between the gravimetric measurements and the Mass measurements on the number of dendron units before and after the HCl digestion seems to suggest that the cross-

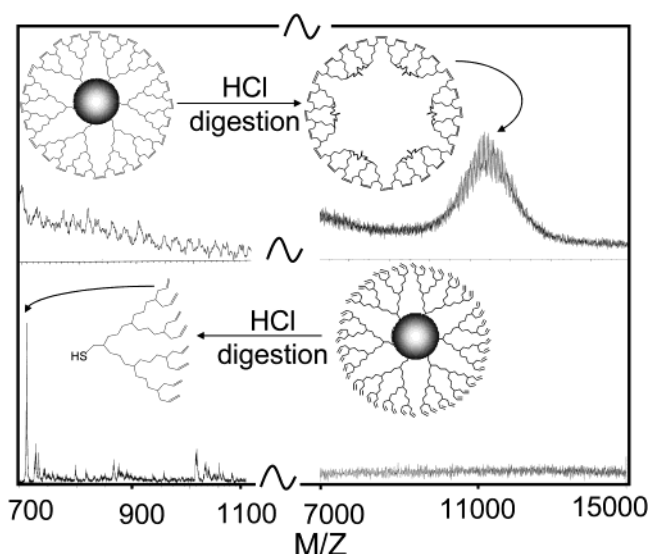


**Figure 3.** Mass spectra of the solutions obtained by the digestion of CdSe dendron-nanocrystals before (bottom) and after (top) the cross-linking reaction.

linking between particles was insignificant. This result is not surprising, given the close packing nature of the double bonds at the outer surface of the ligands monolayer on each nanocrystal and the relatively low molar concentration of the nanocrystals. After cross-linking, the TEM pictures of nanocrystals were almost identical to the ones before the cross-linking, with the majority of the box-nanocrystals far away from each other and a small fraction of the particles only separated by a distance approximately equal to the thickness of two monolayers of ligands. This implies that interparticle cross-linking cannot be completely ruled out although it is unlikely.

This gravimetric method was also used for the determination of the number of dendron ligands on the surface of the dendron-nanocrystals before the cross-linking. The number of dendrons on the surface of the nanocrystals seemed to be related to the reaction temperature in the ligands replacement step although we have not found an optimal condition to control it yet. After the cross-linking reaction, the number of the dendron units on each box-nanocrystal was found typically 10–30% less than that of the dendron ligands of the original dendron-nanocrystals. At this point, it is not clear why this happened.

**Upon the Exposure to a Strong Acid.** HCl (pH = 1.5), the CdSe dendron-nanocrystals decomposed immediately and the inorganic nanocrystals precipitated out of the solution (Figure 4, top-left). The first absorption peak of the solid residual was drastically shifted to blue, indicating a significant shrinkage of the inorganic nanocrystals. However, it took about 2 h for the corresponding CdSe box-nanocrystals to precipitate. As shown in Figure 4 bottom-left, only a few nanometers blue-shift of the first absorption peak was detected within twenty minutes of the acid etching reaction.

In comparison, the core/shell nanocrystals were somewhat more stable for both dendron-nanocrystals and box-nanocrystals, at least for the relatively short time exposures. The precipitation of the CdSe/CdS core/shell dendron nanocrystals occurred after a few minutes of the exposure to HCl. The CdSe/CdS core/shell box-nanocrystals did not show any noticeable blue-shift within 20 min of the exposure.

(39) Schultz, L. G.; Zhao, Y.; Zimmerman, S. C. *Angew. Chem., Int. Ed. Engl.* **2001**, *40*, 1962–1966.

(40) Yu, W. W.; Peng, X., to be submitted.

The size of the inorganic core at the precipitation point of the plain CdSe nanocrystals in both cases was about 2.5 nm. The size of the original nanocrystals was about 3.3 nm. This means that the precipitation occurred when about one monolayer of CdSe was removed from the inorganic nanocrystals. For the core/shell box-nanocrystals, the precipitation also occurred after about one monolayer of CdS was etched away by HCl.

**Strong Oxidant.**  $\text{H}_2\text{O}_2$  (0.15 mol/L), was found to etch both CdSe and CdSe/CdS nanocrystals. The dendron-nanocrystals were much less stable than the corresponding box-nanocrystals when they were exposed to  $\text{H}_2\text{O}_2$ . Figure 5 illustrates the stability of the nanocrystals by plotting the change of the absorbance at the first absorption peak of the original samples. For plain CdSe nanocrystals, oxidation of the nanocrystals was immediately detected for the dendron-nanocrystals and the inorganic nanocrystals precipitated after about 5 min in the  $\text{H}_2\text{O}_2$  solution. The CdSe box-nanocrystals were significantly more stable than the corresponding dendron-nanocrystals although the oxidation of the inorganic core was also observed. Precipitation of the nanocrystals occurred after the reaction proceeded for about 35 min in the case of the CdSe box-nanocrystals.

The CdSe/CdS core/shell nanocrystals were generally more stable than the corresponding plain core nanocrystals. Especially, the core/shell box-nanocrystals did not show any detectable change upon the exposure to  $\text{H}_2\text{O}_2$  at this concentration for at least several hours.

The size of the nanocrystals at the precipitation point in this test was found to be about one monolayer smaller than the original nanocrystals, which is similar to the case of the HCl etching mentioned above.

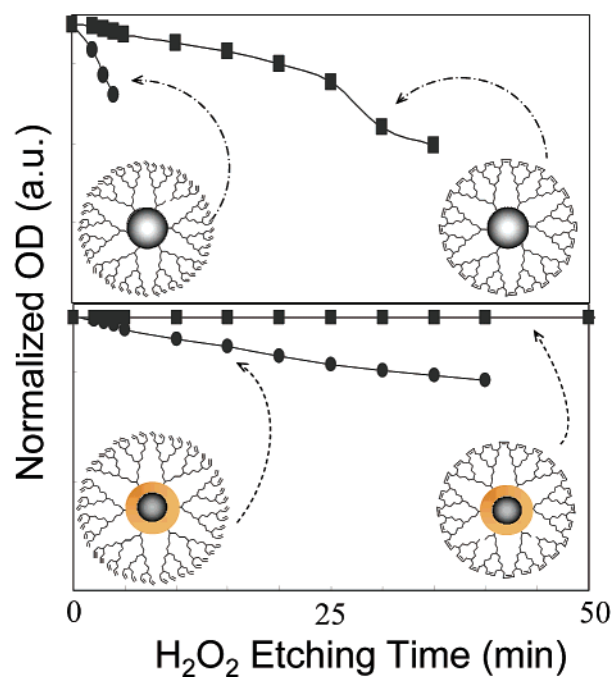


**Figure 5.** Temporal evolution of the optical density (OD) at the first absorption peak of the original nanocrystals in  $\text{H}_2\text{O}_2$  solution.

**Thermal Stability.** The thermal stability of the nanocrystals was examined by sintering the purified nanocrystal powder at 100 °C for about 1 h under vacuum. Except the sintering process, the purification, storage and other processes were all handled in air under ambient conditions. It is known that

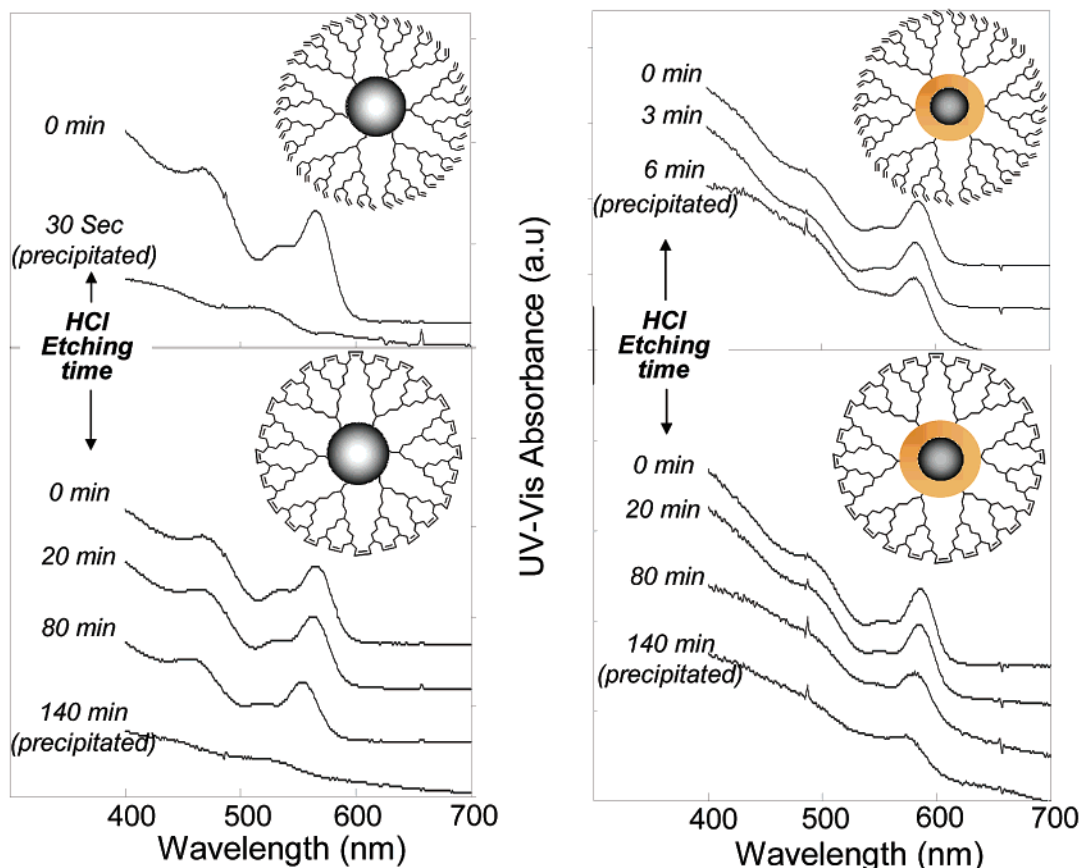


**Figure 4.** Temporal evolution of the UV-vis spectra of the nanocrystals with different inorganic and/or ligands structures etched by HCl solution.

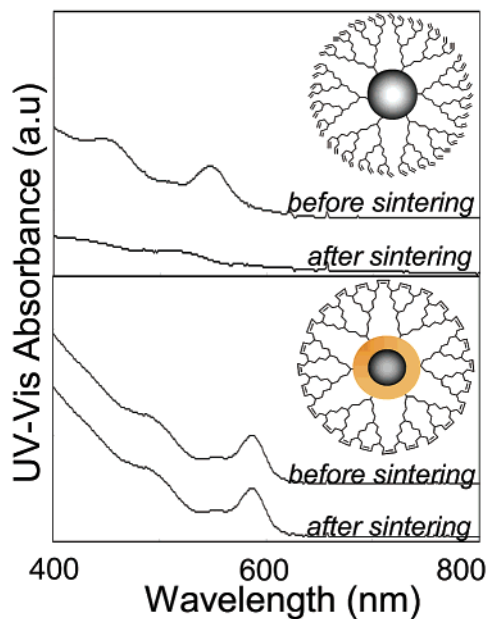


**Figure 6.** UV-vis spectra of the solutions of nanocrystals after and before sintering at 100 °C under vacuum.

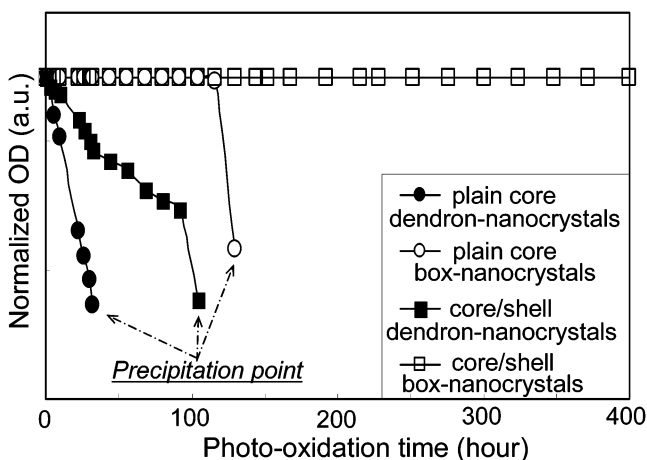


**Figure 7.** Photochemical stability (under UV radiation) of the nanocrystals in air.

nanocrystals coated by typical commercial ligands can barely survive the purification process, including repeated dissolution, precipitation and drying, in air. We previously reported that dendron-nanocrystals can survive those routing treatments without significantly change the solubility of the nanocrystals.

The plain core CdSe dendron-nanocrystals did not survive the harsh heating treatment although it could be dried in a vacuum at room temperature. After the sintering, CdSe dendron-nanocrystals became insoluble in typical solvents (Figure 6). In comparison, the solubility of the CdSe box-nanocrystals, the core/shell dendron-nanocrystals and the core/shell box-nanocrystal was all well maintained, and no any change of the absorption and PL of the nanocrystals was detected for all three samples.

**Photochemical Stability.** The photochemical stability of the nanocrystals in air under UV radiation was studied following the established procedure.<sup>14,15</sup> Figure 7 illustrates the results for four different samples, CdSe dendron-nanocrystals, CdSe box-nanocrystals, CdSe/CdS core/shell dendron-nanocrystals, and CdSe/CdS core/shell box-nanocrystals.

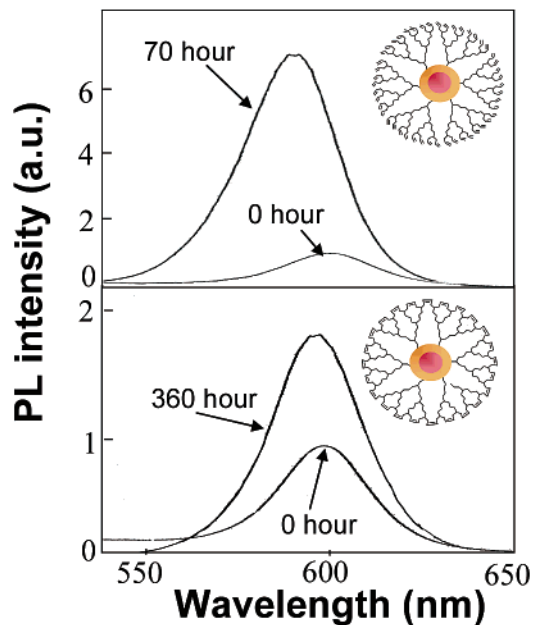


**Figure 8.** Intensity increase and blue shift of the PL spectra of the nanocrystals upon photooxidation.

Evidently, the dendron-nanocrystals of the current ligand system were moderately stable against photo-oxidation. The plain CdSe dendron-nanocrystals were gradually photo-oxidized (Figure 7), and precipitated out of the solution in about 35 h. The CdSe/CdS core/shell dendron-nanocrystals were significantly more stable than the plain core dendron-nanocrystals, and its precipitation occurred after about 100 hours inside the photo-oxidation chamber.

The box-nanocrystals of both plain core and core/shell nanocrystals were much more stable than the corresponding dendron-nanocrystals. For the plain core box-nanocrystals, there was no observable oxidation of the inorganic core detected after the sample was in the photo-oxidation chamber for about 125 h although the precipitation was observed quite rapidly. In the case of the core/shell box-nanocrystals, the photo-oxidation was not detected for 27 d (650 h). After 27 d exposure in the photo-oxidation chamber, the precipitation of the nanocrystals occurred in a rapid fashion which was very similar to that of the CdSe box-nanocrystals shown in Figure 7. The precipitation point of the core/shell box-nanocrystals did not show in Figure 7 because of its different time scale.

**PL.** The PL of the original core/shell nanocrystals was partially remained, about 20% of the original value, after the replacement of the surface amine ligands by the thiol-based dendrons as shown in Figure 1. The cross-linking and the thermal sintering under vacuum did not change the emission properties of the core/shell dendron-nanocrystals and the box-nanocrystals. However, the PL properties of the core/shell nanocrystals were varied in an interesting fashion by the chemical oxidation and photo-oxidation. The PL brightness decreased slightly at the beginning. After this initial stage, the PL brightness often increased significantly (Figure 8), at least with a 2-folds of increase of the relative intensity of the PL peak. The increase of the PL brightness was found always associated with a slight blue shift of the absorption spectra (Figure 8). A similar PL brightening was also observed if the core/shell dendron-nanocrystals were stored in air with room light after several weeks.

The PL properties of the core/shell box-nanocrystal treated under the above chemical oxidation conditions, and the photo-oxidation conditions within approximately 10 days did not show very significant change although some fluctuation was observed, within 20–30% relative intensity variation. However, if the core/shell box-nanocrystal was treated by highly concentrated H<sub>2</sub>O<sub>2</sub> solution, about 100% increase of the PL intensity of the nanocrystals was observed along with a few nanometer blue-shift of the absorption spectrum. It should be pointed out that, with the same concentrated H<sub>2</sub>O<sub>2</sub> solution, the core/shell dendron-nanocrystals were precipitated out of the solution almost instantaneously. Prolonged photo-oxidation (more than about 10 days under the given conditions) was also able to slowly enhance the PL of the core/shell box-nanocrystals (Figure 8). The photobrightening of the PL of core/shell box-nanocrystals under ambient conditions was not observed, likely because it would be extremely slow.

In general, the PL brightening of core/shell nanocrystals through photooxidation was easier to be controlled than that by chemical oxidation, and it was easier to achieve the PL brightening for the core/shell dendron-nanocrystals than for the core/shell box-nanocrystals (Figure 8). It was found that the relative PL efficiency after the brightening could be even higher than the original core/shell nanocrystals coated by amines in organic solvent. If the oxidation process was stopped, the brightened nanocrystals would maintain their PL efficiency at the stop point. In this way, the PL quantum yield of the brightened core/shell dendron-nanocrystals could be stabilized at about 20% to 30%. This brightening phenomenon is in further study and the details will be published later.

The plain core nanocrystals, including the dendron-nanocrystals and the box-nanocrystals, did not emit as soon as the original surface ligands were replaced by the thiol based dendron ligands (Figure 1). This was true even if those highly luminescent CdSe nanocrystals isolated at the “bright point” in a growth reaction<sup>22</sup> were employed for the surface replacement. In addition, all following treatments, including cross-linking, thermal sintering, chemical oxidation and photochemical oxidation, did not bring back noticeable PL for the nanocrystals.

## Discussions

RCM has been widely used for the cross-linking of the branches of dendrimers and the resulting structures are called dendrimer boxes.<sup>36–38</sup> In some cases, the core of the dendrimer box was chemically removed to form an empty box.<sup>36,38</sup> Those dendrimer boxes are being tested as molecular imprinting structures<sup>38</sup> and drug delivery carriers.<sup>37</sup> In the case of semiconductor nanocrystals, Grubbs' catalysts were also employed to build up a thick ligands layer around each semiconductor nanocrystal by the extension of the chain length of each ligand.<sup>41</sup> The results shown in this work revealed that the versatile feature of Grubbs' catalysts can also be exploited to form a thin but globally cross-linked ligand monolayer on the surface of each semiconductor nanocrystal.

The size distribution of those empty dendron boxes revealed by mass spectroscopy (Figure 3) was quite narrow. Typically, the full width at the half-maximum (fwhm) of the mass peak was about 2–4 dendron units, which corresponded to about

5–10% standard deviation in size. This distribution matched quite well with the size distribution of the nanocrystals sealed inside the boxes. From this information, it should be safe to conclude that the surface coverage of the dendron ligands among a batch of nanocrystals was very uniform although they might vary from batch to batch and depend on the reaction conditions as mentioned above. The cross-linking reactions also did not affect this uniformity though 10–30% loss of the dendrons was observed in the cross-linking process.

It is well documented that relatively large species can diffuse in to and out of a dendrimer box. In fact, this permeability is needed for both drug delivery and molecular imprinting. For example, a recent report revealed that the original porphyrin core of dendrimer-boxes could easily be removed by simply cutting the chemical bonds between the core and its peripheral.<sup>38</sup> Furthermore, a slightly smaller but rigid porphyrin molecule could readily squeeze into the empty box. This phenomenon was considered as a new route toward molecular imprinting. In the current report, it was observed that the inorganic nanocrystals could escape the dendron boxes after the chemical bonds between the inorganic nanocrystals and the ligands boxes were destroyed. It would be interesting to see if the empty dendron-boxes generated using nanocrystals as the core could be used for molecular imprinting. To our knowledge, they are likely the largest empty dendron boxes with a narrow size distribution. In the contrast to the large cavity of the box, the wall of the box is quite thin, which is based on a G3 dendron. All of these structural features may be of interest for molecular imprinting and other types of applications in the field of host–guest chemistry. Prior to this work, Wu et al.<sup>42</sup> attempted to obtain nanometer sized polymer capsules through RCM, using Au nanocrystals as the templates and a thiol molecule with three double bonds as the ligands. They noticed that the NMR signals became very sharp after the inorganic cores were removed, which is different from our observations mentioned above. The Au nanocrystals used in their case were about 5 nm in size. If a global cross-linking occurred, the resulting empty capsules should possess a significantly higher molecular mass than that observed in this work, i.e., between 10 000 and 50 000 Dalton. Typically, the peaks of the NMR spectra of such large sized species should be very broad at room temperature, instead of sharp ones observed in their case. Likely, only three double bonds per ligand in their case might not be enough to globally cross-link all ligands of a given nanocrystal. Unfortunately, they only reported some AFM measurements and NMR results of the capsules. It is difficult to judge in what degree they obtained the desired capsules.

Despite the decrease of the thickness of the ligand monolayer, the stability of the box-nanocrystals against harsh chemical, thermal and photochemical treatments was proven dramatically better than that of the corresponding dendron-nanocrystals. These results are consistent with the mechanism of the photo-oxidation of semiconductor nanocrystals, which suggested that the diffusion of active oxygen species is the rate determining step.<sup>14</sup> On the basis of the data obtained in the studies of chemical stabilities of the dendron-nanocrystals and box-nanocrystals, it is reasonable to conclude that diffusion of the

(41) Skaff, H.; Ilker, M. F.; Coughlin, E. B.; Emrick, T. *J. Am. Chem. Soc.* **2002**, *124*, 5729–5733.

(42) Wu, M.; O'Neill, S. A.; Brousseau, L. C.; McConnell, W. P.; Shultz, D. A.; Linderman, R. J.; Feldheim, D. L. *Chem. Commun.* **2000**, 775–776.



small reactants into the nanocrystal-ligands interface was also the rate determining step for those related reactions.

The superior stability of CdSe/CdS core/shell box-nanocrystals against both photo-oxidation and chemical oxidation was expected. The electronic confinement of both photogenerated hole and electrons inside the core material—CdSe in this case—should efficiently suppress photo-oxidation of the CdS shell as reported previously.<sup>34</sup> In terms of chemical oxidation, the oxidation of  $\text{Se}^{2-}$  should be much easier than that of  $\text{S}^{2-}$  based on common chemical knowledge.<sup>43</sup> Consequently, CdSe/CdS core/shell nanocrystals should be more stable against chemical oxidation than CdSe plain core nanocrystals.

The understanding of the better stability of core/shell nanocrystals against thermal sintering in solid state and acid etching in solution is somewhat complicated. Our experimental results revealed that, in solution, the bonding strength between thiol ligands and either CdSe or CdS nanocrystals is very similar.<sup>44</sup> If the bonding situation in solid state at elevated temperature did not change, then the related stability of the two types of nanocrystals should be identical if their ligands layer was the same. Evidently, this is not consistent with the experimental results. Thermodynamically, the stability against HCl etching of the nanocrystals should be related to the precipitation product of the inorganic crystals exposed to the solution, given the similar bonding strength of the thiol ligands with either CdSe or CdS nanocrystals. If thermodynamic factor played a dominating role, then the etching of CdSe/CdS core/shell nanocrystals should be faster than that of the CdSe core nanocrystals, which is not consistent with the experimental results.

The excellent thermal stability of the box-nanocrystals indicates that the irreversible aggregation in solid state of colloidal nanocrystals can be very efficiently stopped by “sealing” each nanocrystal inside a dendron box. In this way, nanocrystals are completely isolated from each other, and it is very difficult for a nanocrystal to escape from its box. This means that the poor purification and storage properties of colloidal nanocrystals could be improved if those nanocrystals were sealed inside desired dendron boxes. More importantly, the performance of the solid state devices made of nanocrystals, such as LEDs and solid state lasers, should be significantly enhanced.<sup>5</sup> In addition, the thin thickness of the ligands monolayer of the box-nanocrystals should also be ideal for efficient charge injection for the solid-state optoelectronic devices. For biological labeling in aqueous solution, some additional development is needed to couple bio-functional groups onto the surface of the box-nanocrystals.

The PL brightening of CdSe/CdS core/shell nanocrystals upon photoradiation can be ascribed to the oxidation of the shell material because it was always associated with a noticeable blue-shift of the absorption spectrum (Figure 8). This conclusion is further supported by the related brightening by the chemical oxidation. In literature, PL brightening phenomena of CdSe/ZnS core/shell nanocrystals were repeatedly reported.<sup>45,46</sup> It is worth to notice that, if ZnS was the shell semiconductor,

oxidation or photo-oxidation of the shell would not affect the peak position of the absorption spectra because of the very high energy band gap of ZnS in comparison to that of either CdS or CdSe. As documented in literature, the absorption peak position of CdSe/ZnS core/shell nanocrystals with one monolayer to seven monolayers of ZnS did not show detectable difference.<sup>47</sup> In our case, because CdS was the shell semiconductor, the slight oxidation of shell could be readily detected by the blue-shift of the absorption spectrum of the core/shell nanocrystals. A more detailed discussion of brightening phenomena will be in another publication.<sup>35</sup>

## Conclusions

The globally cross-linking of the dendron ligands on the surface of the nanocrystals practically sealed each nanocrystal inside a dendron box, which resulted in very stable box-nanocrystals. When the inorganic nanocrystals inside the boxes were CdSe/CdS core/shell nanocrystals, the box-nanocrystals possessed superior stability against chemical, photochemical, and thermal treatments. The luminescence brightness of the core/shell nanocrystals could be partially remained after they were embedded inside the boxes. Furthermore, the luminescence efficiency could be further enhanced by controlled chemical or photochemical oxidation of the nanocrystals. The luminescent core/shell nanocrystals described in this work should be sufficient for the development of many important applications based on semiconductor nanocrystals. The extremely stable box-nanocrystals should be ideal species for studying size dependent chemical and physical properties of high quality semiconductor nanocrystals. The stabilization strategy presented here should be possible to be extended to other colloidal nanocrystal systems, provided that the chemistry involved is reasonably simple and standardized in the literature. The cavity at the center of an empty dendron box formed by the dissolution of the inorganic nanocrystal core in concentrated strong acid is nanometer sized and with a very thin shell. Those nanometer sized capsules ion represent a new class of mesoporous structures, which are soluble in certain solvents and have a very narrow size distribution. Those mesoporous capsules could be of great importance for guest–host chemistry, such as for drug delivery and molecular imprinting.

**Acknowledgment.** Financial support from the NSF and the University of Arkansas is acknowledged. J.J.L. is grateful for the Research Assistant Fellowship provided by Center for Sensing Technology And Research (C-STAR) at the University of Arkansas. Y.A.W. thanks for the support from the “seeds” program of the UA-OU Joint MRSEC.

JA028469C

- (45) Mattoussi, H.; Mauro, J. M.; Goldman, E. R.; Anderson, G. P.; Sundar, V. C.; Mikulec, F. V.; Bawendi, M. G. *J. Am. Chem. Soc.* **2000**, *122*, 12 142.  
(46) Manna, L.; Scher, E. C.; Li, L.-S.; Alivisatos, A. P. *J. Am. Chem. Soc.* **2002**, *124*, 7136–7145.  
(47) Dabbousi, B. O.; RodriguezViejo, J.; Mikulec, F. V.; Heine, J. R.; Mattoussi, H.; Ober, R.; Jensen, K. F.; Bawendi, M. G. *J. Phys. Chem. B* **1997**, *101*, 9463–9475.

(43) Cotton, A. M. *Adv. Inor. Chem.* 1997.

(44) Aldana, J.; Peng, X., in preparation.